

New Frontiers in Retinal Imaging

Zizhong Hu, Qinghuai Liu, Yannis M. Paulus

Zizhong Hu, Yannis M. Paulus, Kellogg Eye Center, Department of Ophthalmology and Visual Sciences, University of Michigan, Ann Arbor, MI, United States of America

Yannis M. Paulus, Department of Biomedical Engineering, University of Michigan, Ann Arbor, MI, United States of America

Zizhong Hu, Qinghuai Liu, Department of Ophthalmology, First Affiliated Hospital of Nanjing Medical University, China

Correspondence to: Yannis M. Paulus, MD, Department of Ophthalmology and Visual Sciences, University of Michigan, Ann Arbor, MI, United States of America.

Email: ypaulus@med.umich.edu

Telephone: +1-734-232-8105

Fax: +1-734-936-3815

Received: June 19, 2016

Revised: July 6, 2016

Accepted: July 9, 2016

Published online: September 18, 2016

ABSTRACT

Ophthalmology is one of the most technology-driven medical specialties with numerous recent advances due to improvements in imaging technology. Advances in retinal imaging have allowed for better understanding of the eye in health and disease, retinal pathophysiology, documenting of disease progression, and assessing therapeutic response. During the last 50 years, both the hardware such as lasers in addition to software image analysis have significantly evolved. These improvements have included facilitating the progress of the ocular examination, reducing the discomfort of patients, and obtaining high quality non-invasive images. This article will review the classic retinal imaging modalities, state-of-the-art retinal imaging technologies, and an introduction of emerging imaging technologies.

© 2016 The Authors. Published by ACT Publishing Group Ltd.

Key words: Retina; Imaging; Fluorescein angiography; Optical Coherence Tomography; Photoacoustic Imaging; Molecular Imaging

Hu Z, Liu Q, Paulus YM. New Frontiers in Retinal Imaging. *International Journal of Ophthalmic Research* 2016; 2(3): 148-158 Available from: URL: <http://www.ghrnet.org/index.php/ijor/article/view/1760>

INTRODUCTION

Retinal imaging plays a very important role in screening the status of the human eye and diagnosing many ocular diseases. In addition to ocular diseases, retinal imaging also allows for early detection, diagnosis, and management of systematic diseases of the brain, endocrine, and cardiovascular systems. The eye is mostly optically transparent, allowing a window into both the central nervous system along with the systemic vasculature.

From the first photograph of human retina in 19th century until today, there have been huge advances in ophthalmic imaging. In the 1950s, modern fundus photography was born with the advent of the electronic flash and 35-mm camera. Later, in the 1960s and 1970s, the introduction of fluorescein^[1] and indocyanine green angiography^[2] revolutionized our ability to assess the integrity of the choroidal and retinal vasculature. The scanning laser ophthalmoscope (SLO) imaging arrived in 1981^[3], followed 10 years later by optical coherence tomography (OCT) imaging^[4]. Since then, a golden age has been heralded in ophthalmic imaging. OCT has released its third generation equipment within 20 years, and the recent emerging OCT angiography (OCTA) has gained clinical popularity.

Other appealing technologies such as adaptive optics and ultra-wide field imaging have been integrated into available retinal imaging modalities, which can significantly improve our image quality and field of view, respectively. These remarkable advances in ophthalmic imaging have transformed the simple photographic documentation into a powerful investigative method enabling clinicians to make objective measurements and assessments of retinal structures in detail. This review introduces the main retinal imaging instruments, their basic principles and current clinical applications, and recent advances in imaging technology.

FUNDUS CAMERA

Since the anterior eye is in the normal state optically transparent, the retina is visible with proper illumination. Somewhat paradoxically, the optical properties of the anterior portions of the eye (such as the cornea and lens) that allow outside image formation make direct inspection of the retina more challenging. Thus, special techniques are needed to obtain a focused image of the retina. Fundus imaging is complicated because illumination and imaging beams cannot overlap,

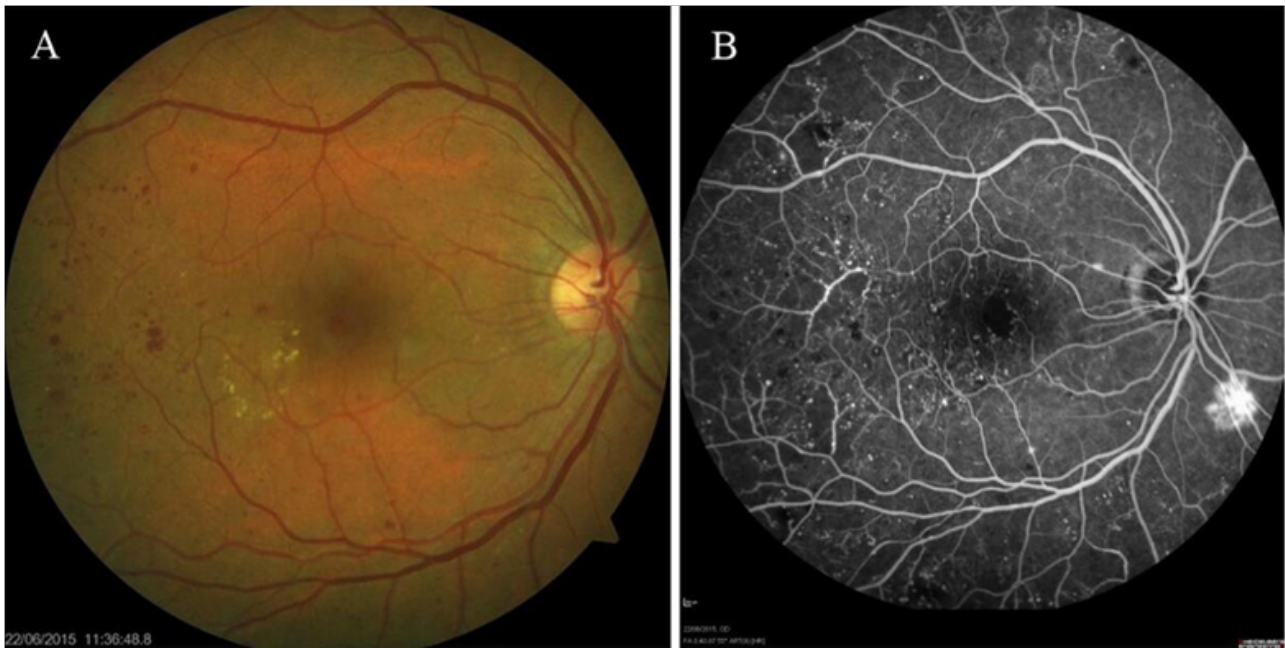


Figure 1 Fundus photography (A) and fluorescein angiography (B) of a patient with diabetic retinopathy.(HRA 2, Heidelberg Engineering, Heidelberg, Germany).

in which case, corneal and lenticular reflections will diminish image quality and contrast.

Consequently, in the pupil plane, separate paths are applied, including an outer illumination beam and an inner imaging beam. The concept of the ophthalmoscope dates back to 1823 by Czech scientist Jan Evangelista Purkyně. It was reinvented by Charles Babbage in 1845^[5,6] and by Hermann von Helmholtz in 1851^[7]. The first attempt to obtain the retinal photography was reported by the Dutch ophthalmologist van Trigt in 1853^[8]. Since then, fundus photography has been a routine ophthalmic examination, with many enhancements, including the transition from film-based to digital image capture, optimization for nonmydriatic image acquisition, and stereoscopic image acquisition^[9,10].

Over the past two decades, efforts have been underway to make the fundus photography more accessible and more robust, with less dependence on experience and expertise. The technology of Picture Archiving and Communication Systems (PACS) allows the fundus camera to move from film-based to digital imaging. More straightforward operation of fundus cameras was further improved due to the development of nonmydriatic imaging and near-infrared focusing, which increased reproducibility. For example, the Nidek Model AFC-230 (Nidek Inc., Fremont, CA), a nonmydriatic fundus camera with a 45-degree field view, has been demonstrated to be an efficient screening tool for diabetic retinopathy in a clinical trial^[11].

In addition, portable, handheld smartphone-based retinal cameras have begun to play an important role as an ocular diagnostic tool and take advantages of the portability, data storage capacity, and wireless telecommunication system built into modern smart phones^[12,13]. Other fundus cameras have been developed which incorporate adaptive optics or ultra-wide field imaging (see below). Combinations of these technologies make fundus photography more appealing and beneficial for the general ophthalmic examination, especially facilitating eye examination in pediatric practice and by nonophthalmic-trained physicians.

FUNDUS ANGIOGRAPHY

As an important extension of the fundus camera, fluorescein angiography (FA)^[1] and indocyanine green (ICG) angiography^[2] have remained integral parts of the clinical evaluation of retinal and choroidal circulations. For FA, blue light with an excitation wavelength of 465 to 490 nm is used. Barrier filters block the light between 465 and 490 nm to block reflected light and allow only the emitted light with a longer wavelength in the yellow-green spectrum at 520-530 nm. As a smaller molecule, fluorescein is not suitable for detailed choroidal imaging due to the profound leakage of dye from fenestrated blood vessels of the choroid (including the choriocapillaris).

Indocyanine green, as a larger molecule, does not leave the choriocapillaris. ICG has been used as a contrast agent for enhanced visualization of the choroidal circulation. FA is a good baseline tool for the diagnosis of neovascular macular degeneration^[14] and diabetic retinopathy^[15] (Figure 1), whereas ICGA complements FA and is mainly used in the diagnosis of polypoidal choroidal vasculopathy (PCV)^[16], choroidal tumors, and choroidal vascular hyperpermeability associated with central serous chorioretinopathy^[17]. Vessel diameter, density, tortuosity, and branching patterns may offer potential value in the future if FA or ICGA can be combined with noninvasive motion contrast image-processing and ultra-wide-field techniques (see below).

SCANNING LASER OPHTHALMOSCOPE (SLO) AND ADAPTIVE OPTICS (AO)

First described in the early 1980s^[3,18], the SLO uses a single, monochromatic laser with low power and a confocal raster scanning technique to collect an image of the retina and optic nerve head. Unlike the fundus camera which produces an image using a film or a charge-coupled device (CCD), SLO systems only illuminate a small area at any one time and the intensity of each pixel is recorded using

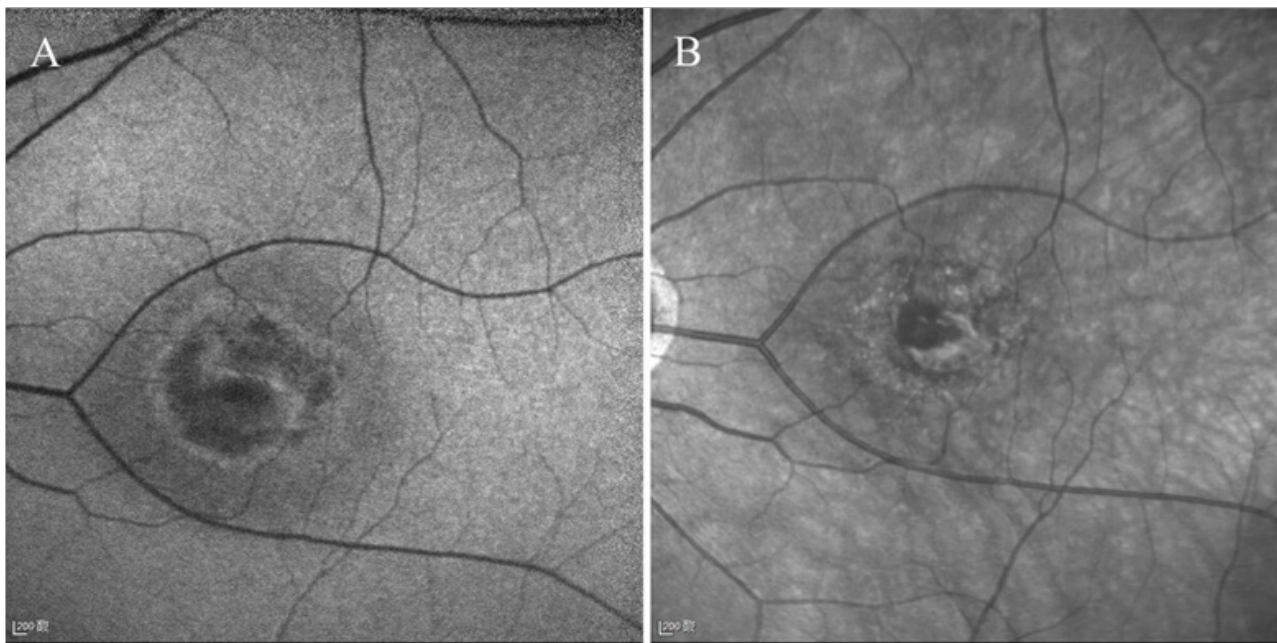


Figure 2 Fundus autofluorescence (A) and near infrared autofluorescence (B) images of a patient with age-related macular degeneration. (HRA 2, Heidelberg Engineering, Heidelberg, Germany).

a single, light sensitive detector. In this sense, the effects of light scatter are reduced so that the output images are with higher contrast than standard fundus cameras. One major advantage of SLO is its ability to perform confocal imaging^[19,20].

Taking advantage of the principle of confocal microscopy, confocal SLO moves a confocal aperture between two end points to obtain a number of tomographic slices and to extract depth information^[21,22]. Confocal SLO and OCT have become standard instruments for scanning the optic nerve head in glaucoma and are widely being used for imaging the RNFL^[23,24]. Another important feature of SLO is the use of different wavelength lasers to enable a pseudo-color fundus image. Such devices, usually called multi-spectral SLOs, employ several laser sources of different wavelengths in the illumination. These multiple laser beams are made coaxial by a set of dichroic mirror and the images are created by a multispectral frame acquisition model. In addition to the pseudo-color fundus image, the changeable laser wavelength of multi-spectral SLOs also allows capture of near infrared reflectance images, fundus autofluorescence (FAF) images, and FA and ICG angiography. This can also be used to perform of retinal vessel oximetry, reflectometry, angioscotometry, fundus perimetry^[25,26,27].

Further improvements of SLOs include time tracking and adaptive optics (AO). For patients who cannot fixate properly (i.e. diabetic retinopathy), high-speed retinal tracking is essential to improve image quality^[28]. To achieve this, retinal spatial information from a fixed frame is used as a reference, and active tracking is performed by placement of a dithered beam originating from a low-power LED onto the fundus. Detection and processing of the backscattered reflectance signals by a phasesensitive detector enhances the imaging capabilities of the SLO.

SLO has been significantly improved through integration to AO, called Adaptive Optics Scanning Laser Ophthalmoscope (AOSLO). AO is used in retinal imaging systems to compensate for optical aberrations through a wave front-sensing technology and a deformable mirror. A wave front sensor, most commonly the Shack-Hartmann sensor, is employed to measure the aberration that the patient's lens, cornea, and tear film introduce in the imaging beam, and the deformable mirror, as a wave front corrector, corrects the

aberration by physically changing its surface shape to compensate that of the aberration measured^[29-32]. AOSLO systems have been reported to have the capability of observation of individual cone and rod photoreceptors^[33,34], blood vessel and capillary imaging^[35-37], and retinal pigment epithelium (RPE) (Figure 2)^[38].

FUNDUS AUTOFLUORESCENCE (FAF)

Fundus autofluorescence (FAF) has grown significantly in popularity over the past decade. FAF is a non-invasive fundus imaging modality which provides information on native fluorescent molecules. The primary FAF signal is lipofuscin that has accumulated in RPE cells. Lipofuscin accumulation is due to deficient digestion of the photoreceptor outer segments by RPE cells. Elevation of lipofuscin in the RPE is indicative of cellular stress and often is a precursor of cell death^[39]. Thus, autofluorescence is increased with RPE dysfunction and is decreased with the loss of photoreceptors and RPE.

Clinical applications of FAF include monitoring the progression of geographic atrophy^[40], diagnosis of Best inherited macular dystrophy^[41,42], intraocular tumors^[43], posterior uveitis^[44,45], and detecting drug toxicity such as hydroxychloroquine retinopathy^[46]. Lipofuscin has a broad range of excitation from 300 to 600 nm, allowing visible light to elicit its fluorescence in the human retina^[47]. Instruments for the measurement of FAF include the fundus spectrophotometer^[48], fundus camera^[49], and cSLO^[47].

One common cSLO is the Heidelberg retinal angiographs (HRA Classic, HRA 2, and Spectralis HRA; Heidelberg Engineering, Heidelberg, Germany). In this system, excitation occurs with a 488 nm illumination and the emission is detected above 500 nm (Figure 2)^[50]. Image averaging occurs automatically and in real-time. In addition, normalization of pixel intensity occurs, which facilitates quantification and comparison between different FAF images^[47]. In addition, near infrared AF (NIR-AF), with an excitation wavelength of 787 nm and an emission of > 800 nm, is capable of imaging the melanin in RPE and choroid layers (Figure 2)^[51,52]. Further, NIR-AF in patients with AMD has been described, using the ICG mode (790 nm as excitation wavelength). The recorded signal is likely melanin-dependent^[52].

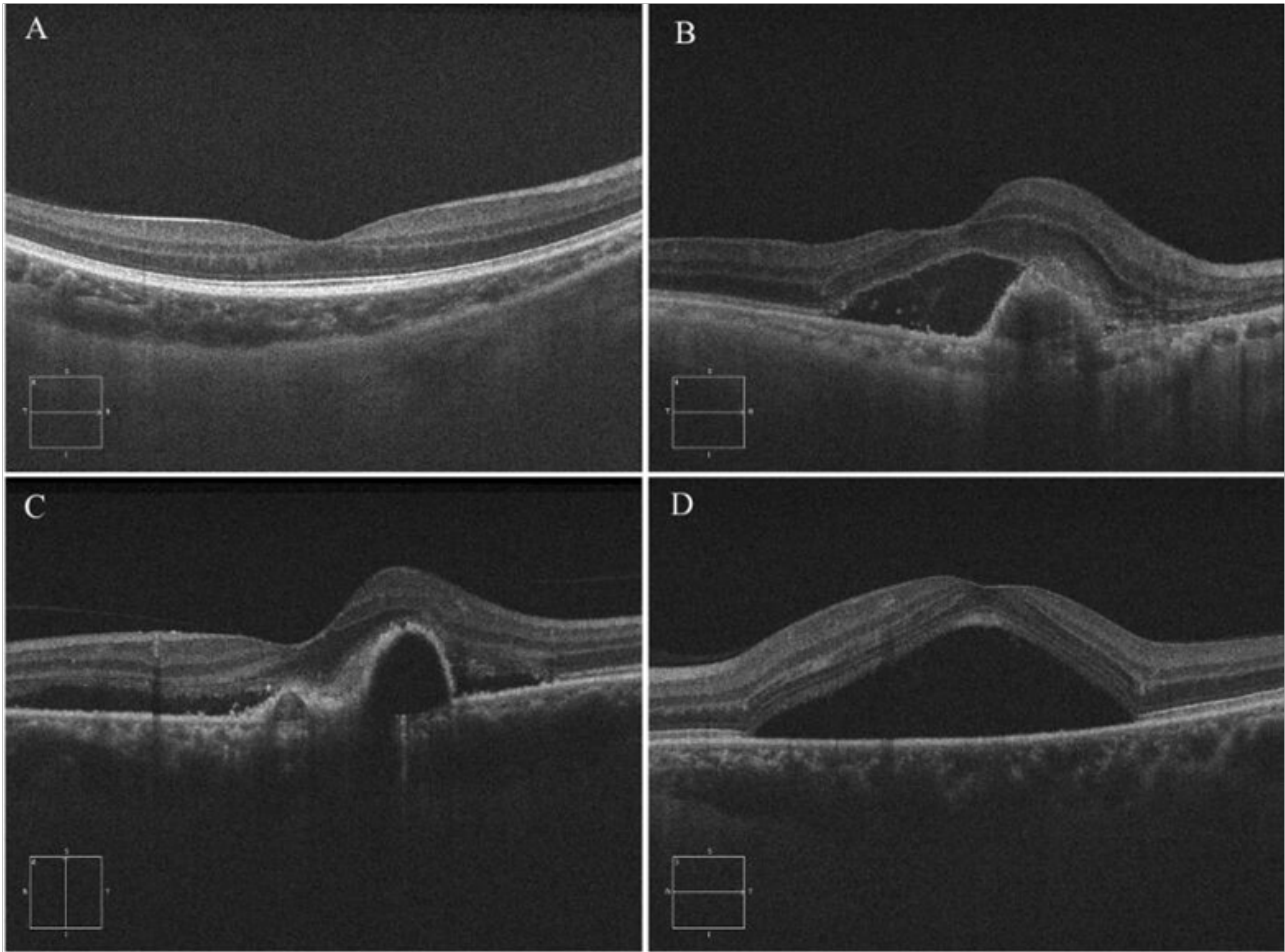


Figure 3 Representative cross-sectional OCT images of a normal fundus (A), wet age-related macular degeneration (B), polypoidal choroidal vasculopathy (C), and central serous chorioretinopathy (D). (Cirrus OCT, Carl Zeiss Meditec, Dublin, CA, USA).

ULTRA-WIDEFIELD IMAGING

The “standard” field of view of the traditional, commercially available fundus camera is 30 to 50 degrees, which correspond to approximately 5% to 15% of the retinal surface area, respectively. With traditional cameras, it is difficult to photograph the peripheral retina. Even with montage techniques, the standard 7 fields cover around 75 degrees. Moreover, certain constraints exist in FA or ICGA in particular, as fluorescence in transit is time-sensitive and different parts of the retina cannot be imaged simultaneously. Imaging angles larger than 50 degrees have been referred to as “wide-field”. More recently, the term “ultra-wide field” (UWF) fundus imaging has gained popularity, although the exact definition and area of the retina imaged remains ambiguous^[53].

Several camera designs were released with different properties. Optos (Optos, PLC, Scotland) increases the field of view up to 200° covering approximately 82% of the retina in a single image. Heidelberg Spectralis (Heidelberg Engineering, Germany) is another UWF camera with a 102° field of view with noncontact lens and 150° with Staurengi contact lens. The Optos captures an appreciably wider view of the retina temporally and nasally, despite of peripheral distortion, while the ultra-wide field Heidelberg Spectralis is able to image the superior and inferior retinal vasculature more peripherally^[53]. Of note, the Heidelberg Spectralis provides a higher resolution image than that of Optos^[23].

Recent advances in UWF imaging software, such as stereographic

projection software, now have been available in commercial UWF devices. This allows images obtained at different gaze angles to be montaged and corrected for peripheral distortion^[54]. Not limited to the fundus camera, UWF has also been employed in other retinal imaging modalities like fundus fluorescein angiography^[55], OCT^[56], autofluorescence^[57], and scanning laser ophthalmoscopy^[58].

OPTICAL COHERENCE TOMOGRAPHY (OCT)

OCT is a powerful imaging system for acquiring cross-sectional images of tissue non-invasively (Figure 3). OCT creates an image based on low-coherence interferometry and analyzes the difference in back-scattered light comparing the tissue to a reference arm^[59]. A broad band light source is first split into two beams: a reference and sample beam. The back-scattered beam from the retina generates an interference pattern with the reference beam. From this, a reflective depth and intensity profile of the retina can be constructed^[4]. Initially, the interference patterns generated in the early OCT systems varied as a function of time using a moving mirror in the reference pathway. Such devices were termed time-domain OCT (TD-OCT)^[60]. TD-OCT systems like Stratus OCT (Carl Zeiss Meditec, Inc., Dublin, CA, USA) acquire image at 400 A-scans per second scan with an axial resolution of approximately 10 μm^[61].

The second generation is spectral-domain OCT (SD-OCT), which employs an interferometer and spectrometer to analyze back-scattered light interference pattern simultaneously through the Fourier transform algorithm^[62,63]. The SD-OCT systems such as the Cirrus

OCT (Carl Zeiss Meditec, Dublin, CA, USA), Spectralis (Heidelberg Engineering GmbH, Heidelberg, Germany), RTVue-100 (Optovue Inc., Fremont, CA, USA), and Topcon 3D-OCT 2000 (Topcon Corporation, Tokyo, Japan) allow much faster scan rates at 20,000 to 52,000 A-scans per second, better signal-to-noise ratio compared with TD-OCT, and a higher axial resolution of 5 to 7 μm ^[62,63].

The third generation OCT, so called swept-source OCT (SS-OCT), alternatively employs a tunable frequency-swept laser light source and a photodetectors to assesses interference patterns^[64]. Such devices as DRI OCT-1, Atlantis (Topcon Corporation, Tokyo, Japan) has an image acquisition speed of 100,000 A-scans per second and ultra-fast SS-OCT with an acquisition speed as high as 6,700,000 A-scans per second^[65]. Another advantage of SS-OCT is the improvement of the signal quality in deep tissue by elimination of the sensitivity of a spectrometer to higher frequency modulation as with SD-OCT, thereby improving the visualization of the choroid^[66]. With the application of longer-wavelength light source—approximately 1,000 nm, the SS-OCT systems are expected to improve the visualization of choroid–sclera interface^[67]. This is very important for the diagnosis of diseases such as central serous chorioretinopathy (CSCR), and pathological myopia, where the thickness of choroid is abnormal. This also improves choroidal volumetric analysis and visualization of various pathological features such as choroidal neovascularization and subretinal/intraretinal fluid.

In addition to the commercially available desktop systems, prototype OCT systems have greatly contributed to an ever-growing body of OCT research field. These include, but are not limited to, the ultra-high resolution OCT (UHR-OCT), handheld OCT, and intraoperative OCT (iOCT). Ultra-high resolution OCT typically employs a broader bandwidth laser of over 100 nm at the wavelength of 830 to 870 nm to provide axial resolutions of 2-3 μm , which reveals retinal morphology in high detail. However, because it requires femtosecond laser and expensive light sources, UHR-OCT has not become widely used in the clinical setting at this time^[68-70].

Handheld OCT, or mobile OCT, may further expand the application spectrum of OCT to help the analysis of subjects who cannot be ambulatory or cooperative, including adults and pediatric patients. Ashwin *et al* in 2015 reported that with a handheld SD-OCT Envisu 2300 (Bioptigen Inc., Research Triangle Park, NC, USA), they studied 975 infants and children^[71]. The handheld SD-OCT can assist with the monitoring and evaluation of hereditary maculopathies^[72,73]. The upgraded handheld OCT is capable of imaging both the anterior and posterior segments of the eye in rapid succession^[74].

Another exciting application of OCT is the potential use of intraoperative OCT (iOCT) during surgery, especially for vitreoretinal surgery. The great advantage of iOCT is to assist with the prompt decision-making process and to allow additional deliberate surgical maneuvers aimed at improving surgical outcomes. Traditional table-top designed OCT systems have been playing an essential role in the diagnosis, treatment, and evaluation of macular diseases^[75]. However, accurate image acquisition with these modalities needs a compliant patient who can sit in an upright position, which is paradoxical considering the intraoperative posturing of patients. With the development of integrative OCT technology, surgical instrumentation, and software algorithms, intraoperative OCT (iOCT) is becoming increasingly utilized.

Three kinds of iOCT have been employed during surgery, which include hand-held SD-OCT devices (for example, iVue, Optovue Inc., Fremont, CA, USA)^[76], microscope-mounted OCT system (Bioptigen Envisu SDOIS; Bioptigen, Research Triangle Park, NC, USA)^[77], and intra-ocular side-scanning OCT endoprobe (C7 System;

Light Lab Imaging, Inc/St Jude Medical, St. Paul, MN, USA)^[78]. Since the current commercially available handheld OCT systems must move the OCT system in and out of the surgical field, the microscope-mounted OCT system and intra-ocular OCT endo probe are more readily incorporated into the surgical field.

DOPPLER OCT

OCT is performed using intrinsic contrast alone, not requiring the use of dyes or extrinsic contrast agents. This non-contrast capability is attractive for longitudinal studies where cumulative dye toxicity is a concern. Since OCT can measure well-defined volumes using predominantly single scattered light, quantitative assessment of hemodynamic parameters such as the diameter of blood vessel and blood flow using Doppler algorithms are possible. Doppler OCT is based on the traditional OCT system with the phase-resolved axial scan information.

Fourier-domain OCT has proven to enable Doppler OCT through simpler and more robust measurements of human retinal blood flow in real time using depth-resolved information on vascular structure and Doppler velocity^[79]. However, the flow measurement was highly sensitive to errors in the Doppler angle, especially when the vessel is nearly vertical to the OCT beam around the optic disc margin. Eye-motion artifacts as well as varied vessel geometries can make the angle measurements challenging and require additional data analysis.

Another method, bidirectional Doppler OCT measures Doppler velocity in two probe beam directions and uses trigonometric relations to calculate the absolute flow velocity^[80] and blood flow^[81]. In addition, the improvement of OCT scan speed enabled another Doppler OCT approach, which analyzes blood flow in the *en face* plane and therefore, avoids the need to measure the Doppler angle^[79]. In ophthalmology, *en face* Doppler OCT does not require the measurement of Doppler angle because the detected flow velocity component is always perpendicular to the *en face* plane. Lee *et al*^[82] suggested that precise measurement of total retinal blood flow using *en face* Doppler OCT at commercially available scan speeds should be feasible while further validation in diseased subjects is required.

OPTICAL COHERENCE TOMOGRAPHY ANGIOGRAPHY (OCTA)

Optical coherence tomography (OCT) angiography (OCTA) is an emerging and promising approach that uses SD-OCT for non-invasive visualizing of retinal and choroidal vessels based on flow rather than simple reflectance intensity. An important advantage of OCTA over traditional fluorescein angiography (FA) is that it provides three-dimensional, depth-resolved functional information of bloodflow in vessels (Figure 4). OCTA works by evaluating the difference between sequential OCT B-scans in the retina. Since the tissue structure does not change in this short interval, change is attributed to movement of erythrocytes within the blood vessel lumen. By applying the key technology of the split-spectrum amplitude decorrelation algorithm (SSADA)^[83], OCT signal is first split into several spectral bands, each of which forms a different speckle pattern. The next step is the sum of amplitude decorrelation images derived from these spectral bands, which increases the flow signal and reduces the image noise.

As OCTA is a depth-resolved technique, precise axial segmentation of retinal layers is needed as to acquire important data on perfused structures and simultaneously. OCTA thus avoids the risk of generating superimposed images, which are typical of FA or ICGA. To achieve this, several methods have been employed. An

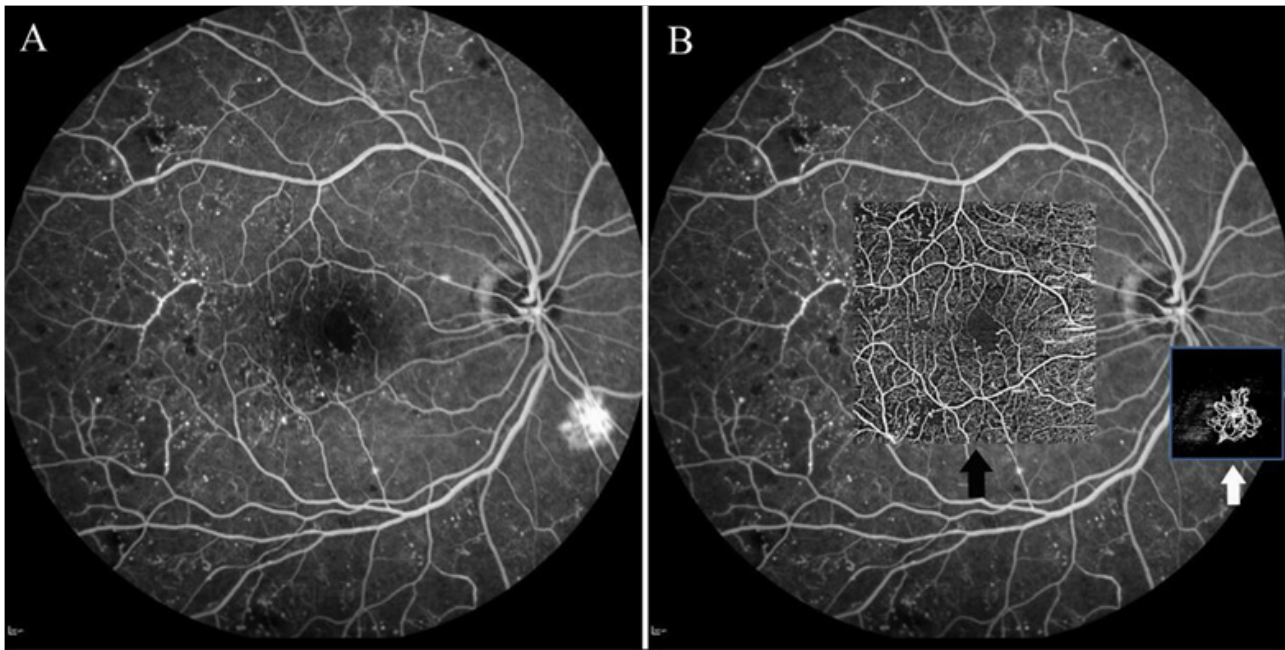


Figure 4 Fluorescein angiography (A) and OCT angiography (B) images of a patient with diabetic retinopathy. OCT angiography showed more detailed information of the macular microvascular structure (white arrow) and indicated the neovascularization (segmentation at the level of vitreous-retinal interface) near the optic head where FA only showed dye leakage. (HRA 2, Heidelberg Engineering, Heidelberg, Germany; ZEISS Angioplex, Carl Zeiss Meditec Inc., Dublin, CA, USA).

automated segmentation algorithm is provided by the majority of different OCTA devices^[84]. This algorithm is capable of providing an extremely fast way to delineate the presence of a decorrelation signal and to distinguish different retinal layers, from the inner limiting membrane (ILM) to the RPE, including the external limiting membrane, ellipsoid zone, and outer segment.

Another case is *manual segmentation*^[84], where the manual selection of C-scans at different depths is performed with either horizontal or variably shaped sections. The horizontal section (not aligned to any retinal layer) can reduce artifacts due to segmentation errors. Despite both methods, a major and unavoidable limitation of OCTA is projection artefacts, in which superficial retinal vessels are projected onto the deep plexuses and choriocapillaris. This can limit the accurate interpretation of vascular pathology in the deeper layers. Other challenges of OCTA include inability to view leakage from vessels like FA or ICGA, limited imaging of slow flow situations such as microaneurysms or fibrotic CNV, a limited field of view (3×3 or 6×6 mm)^[85], and eye motion artifacts^[86].

The currently commercially available OCTA systems used in clinic include the Angio Vue Imaging System (Optovue, Inc., Fremont, CA)^[87], ZEISS Angioplex (Carl Zeiss Meditec Inc., Dublin, CA, USA), Swept-Source Optical Coherence Tomography Angio (Topcon Corporation, Tokyo, Japan), and Heidelberg Spectralis (Heidelberg engineering, Heidelberg, Germany). OCTA has been playing an active role in the evaluation of common ophthalmologic diseases such as diabetic retinopathy (DR), age related macular degeneration (AMD), artery and vein occlusions, and glaucoma. OCTA has been demonstrated to visualize areas of retinal non-perfusion^[88,89] and the foveal avascular zone (FAZ) of the retinal capillaries^[90], which are essential to describe the DR progression^[91].

OCTA has also been reported to be sensitive in detecting Type I^[92], Type II^[93], and Type III^[94] choroidal neovascularization (CNV) in AMD patients. Furthermore, OCTA has been suggested to visualize alterations in the choriocapillaris of patients from dry AMD^[95,96]. For retinal vein occlusions (RVO), Kashani *et al* reported findings

in OCTA of 26 eyes with RVO that were consistent with clinical, anatomic, and fluorescein angiographic findings including areas of impaired vascular perfusion, retinal atrophy, vascular dilation, shunt vessels, and some forms of intraretinal edema^[97]. Researchers also demonstrated the usefulness of OCTA in evaluating the response to anti-VEGF treatment^[98,99]. OCTA has been demonstrated to be useful to identify the retinal vascular pathology in diseases such as macular telangiectasia Type 2^[100], sickle cell retinopathy^[101], central serous chorioretinopathy (CSCR)^[102], and glaucoma^[103].

OCTA represents a promising emerging retinal imaging modality that can potentially be applied in the screening, monitoring and treatment of retinal diseases. Most of the current literature describing OCTA has been small cross sectional studies. Thus, larger, prospective, randomized clinical trials are required. Establishing a normative and pathologic database and evaluating the sensitivity and specificity of OCTA is important for an emerging technology. It is also important to evaluate the clinical applications of OCTA in assessing therapeutic effects of various treatment strategies in retinal and choroidal diseases. Additionally, considering its limitations, future improvements in OCTA may focus on new algorithms that maximize signal-to-noise-ratio, new OCT devices with faster scanning speed to expand the field of view, and eye-tracking system to decrease eye motion artifacts.

PHOTOACOUSTIC IMAGING

As a hybrid biomedical imaging method, photoacoustic (PA) imaging exploits both optical and acoustical properties and provides functional and structural information of bio-tissues. A nanosecond pulse-duration laser beam is employed to irradiate the target tissue of interest, causing photons to propagate inside the tissue. Absorption of these photons leads to a slight localized transient temperature rise of the tissue, followed by a transient thermoelastic expansion. Ultrasonographic pressure waves, called PA waves, can then be induced by the transient thermoelastic expansion, detected by

broadband ultrasonic transducers, and imaged^[104].

In the eye, the major light-absorbing materials are hemoglobin inside the blood vessels and melanin inside the RPE and choroid. PA offers the first possibility for direct measurement of light absorption by retinal tissues. PA can be a potential tool for noninvasive and sensitive imaging of retinal and choroidal structures^[105]. Apart from the photoacoustic tomography (PAT) used to visualize the entire eye^[106,107], photoacoustic ophthalmoscopy (PAOM) is emerging as a promising tool. With the guidance of OCT, PAOM has been reported to be capable of image the retinal vessels^[108,109,110], RPE cells^[109,110], and choroidal vessels^[108,110] in rodent animals with a axial resolution of around 20 μm ^[111,112] and a higher resolution that can reach 4 μm ^[112,113].

In addition, photoacoustic imaging provides a new method to accurately sense oxygen saturation through direct measurement of light absorption within blood with multiple laser wavelengths^[114]. In future research, PAOM can be improved in terms of its resolution, use of contrast agents for molecular imaging, and harmonious integration with existing fundus imaging modalities.

MOLECULAR IMAGING

Although ophthalmic imaging modalities are capable of imaging retinal morphology with unprecedented resolution, challenges still remain to detect subclinical molecular changes. Subclinical changes are subtle cellular and molecular changes which occur before retinal disease can be detected by current anatomy-driven ophthalmic imaging instrumentations. Molecular imaging includes strategies capable of detecting disease biomarkers in the retina. Two important components of retinal molecular imaging are the potential biomarkers to be targeted and the molecular profiling techniques to be employed. A number of studies have reported feasibility of molecular imaging in detecting retinal ganglion cells (RGCs), RPE cells, endothelial cells, and leukocytes.

Cordeiro *et al*^[115,116] used molecular imaging technology named detection of apoptosing retinal cells (DARC) for the single-cell detection of RGC apoptosis, where Annexin V was intravitreally injected to specifically bind the apoptosis biomarker phosphatidylserine (PS) and then was detected by ophthalmic fluorescence imaging instrumentation. Barnett *et al*^[117] utilized a peptide-based fluorescent probe (TcapQ) which is sensitive to active caspases such as caspase 3 involved in RGC apoptosis to *in vivo* quantify apoptotic RGCs. Another promising opportunity for molecular imaging of RGCs lies in the imaging of RGC dysfunction before cell death. Several imaging probe such as reactive oxygen (ROS)^[118], mitochondria selective JC-1^[119], and E glutamate^[120] hold great promise in improving the molecular imaging of RGCs.

Beyond autofluorescence imaging, several RPE-related molecular targets may also warrant consideration, such as ROS^[121], β -amyloid, esterified cholesterol and carbohydrate moieties in drusen^[122]. As for endothelial cells, the surface biomarkers of inflammation or angiogenesis are potential candidates for development of targeted contrast agents for ophthalmic imaging of retinal or choroidal neovascularization. The C-C chemokine receptor 3 (CCR3) is a promising biomarker of choroidal neovascularization (CNV), as demonstrated by CCR3 expression on choroidal neovascular endothelial cells in human CNV specimens^[123].

Other promising biomarkers include targeting proliferating endothelial, endoglin^[124], and integrin $\alpha_v\beta_3$ ^[125,126]. These have been successfully imaged in patient specimens *ex vivo* and in cardiovascular diseases and cancer. While currently in its infancy,

molecular imaging of the retina will likely play a critical role in disease diagnosis and monitoring in the future.

CONCLUSIONS

Ophthalmic imaging has rapidly developed and advanced during the last 30 years. Traditional fundus camera and FA/ICGA still play pivotal roles in disease diagnosis and monitoring. Integrated technologies with previously developed retinal imaging instruments such as hand-held, ultra-wide field, and adaptive optics have improved and transformed our imaging capabilities. The non-invasive OCT and OCTA also have further profound benefits in providing improved resolution anatomic imaging, intraoperative surgical planning, and expanding scan area. Finally, photoacoustic imaging and molecular imaging are novel fields in their infancy, which will likely play a larger and more critical role in the future through providing a window on dynamic disease processes, such as inflammation, apoptosis, and neovascularization. Ophthalmic imaging will continue to rapidly advance and result in improved patient care for years to come.

CONFLICT OF INTERESTS

The authors declare that they do not have conflict of interests.

REFERENCES

1. Novotny HR, Alvis DL. A method of photographing fluorescence in circulating blood in the human retina. *Circulation* 1961; **24**: 82-86
2. Flower RW, Hochheimer BF. Clinical infrared absorption angiography of the choroid. *Am J Ophthalmol* 1972; **73**: 458-459
3. Webb RH, Hughes GW. Scanning laser ophthalmoscope. IEEE transactions on bio-medical engineering 1981; **28**: 488-492
4. Huang D, Swanson EA, Lin CP, Schuman JS, Stinson WG, Chang W, Hee MR, Flotte T, Gregory K, Puliafito CA, Fujimoto JG. Optical coherence tomography. *Science (New York, NY)* 1991; **254**: 1178-1181
5. Flick CS. Centenary of Babbage's ophthalmoscope. *The Optician* 1947; **113**: 246
6. Keeler CR. 150 years since Babbage's ophthalmoscope. *Archives of ophthalmology (Chicago, Ill: 1960)* 1997; **115**: 1456-1457
7. Pearce JM. The ophthalmoscope: Helmholtz's Augenspiegel. *European Neurology*, (2009).
8. Trigt, Van ACTaR. Dissertatio ophthalmologica inauguralis de speculo oculi. (1853).
9. Bennett TJ, Barry CJ. Ophthalmic imaging today: an ophthalmic photographer's viewpoint - a review. *Clinical & experimental ophthalmology* 2009; **37**: 2-13
10. Bursell SE, Cavallerano JD, Cavallerano AA, Clermont AC, Birkmire-Peters D, Aiello LP, Aiello LM; Joslin Vision Network Research Team. Stereo nonmydriatic digital-video color retinal imaging compared with Early Treatment Diabetic Retinopathy Study seven standard field 35-mm stereo color photos for determining level of diabetic retinopathy. *Ophthalmology* 2001; **108**: 572-585.
11. Ryan ME, Rajalakshmi R, Prathiba V, Anjana RM, Ranjani H, Narayan KM, Olsen TW, Mohan V, Ward LA, Lynn MJ, Hendrick AM. Comparison Among Methods of Retinopathy Assessment (CAMRA) Study: Smartphone, Nonmydriatic, and Mydriatic Photography. *Ophthalmology* 2015; **122**: 2038-2043
12. Rajalakshmi R, Arulmalar S, Usha M, Prathiba V, Kareemuddin KS, Anjana RM, Mohan V. Validation of Smartphone Based Retinal Photography for Diabetic Retinopathy Screening. *PLoS One* 2015; **10**: e0138285

13. Maamari RN, Keenan JD, Fletcher DA, Margolis TP. A mobile phone-based retinal camera for portable wide field imaging. *The British journal of ophthalmology* 2014; **98**: 438-441
14. Rishi P, Bhende M, Sen P, Rishi E. Discrepancy between fluorescein angiography and optical coherence tomography in detection of macular disease. *Retina* 2009; **29**: 121
15. Silva PS, Dela Cruz AJ, Ledesma MG, van Hemert J, Radwan A, Cavallerano JD, Aiello LM, Sun JK, Aiello LP. Diabetic Retinopathy Severity and Peripheral Lesions Are Associated with Nonperfusion on Ultrawide Field Angiography. *Ophthalmology* 2015; **122**: 2465-2472
16. Cheung CM, Lai TY, Chen SJ, Chong V, Lee WK, Htoon H, Ng WY, Ogura Y, Wong TY. Understanding indocyanine green angiography in polypoidal choroidal vasculopathy: the group experience with digital fundus photography and confocal scanning laser ophthalmoscopy. *Retina* 2014; **34**: 2397-2406
17. Pang CE, Shah VP, Sarraf D, Freund KB. Ultra-widefield imaging with autofluorescence and indocyanine green angiography in central serous chorioretinopathy. *Am J Ophthalmol* 2014; **158**: 362-371.e362
18. Webb RH. Optics for laser rasters. *Applied optics* 1984; **23**: 3680
19. Webb RH, Hughes GW, Delori FC. Confocal scanning laser ophthalmoscope. *Applied optics* 1987; **26**: 1492-1499
20. Sharp PF, Manivannan A. The scanning laser ophthalmoscope. *Physics in medicine and biology* 1997; **42**: 951-966
21. Vieira P, Manivannan A, Lim CS, Sharp P, Forrester JV. Tomographic reconstruction of the retina using a confocal scanning laser ophthalmoscope. *Physiological measurement* 1999; **20**: 1-19
22. Sharp PF, Manivannan A, Vieira P, Hipwell JH. Laser imaging of the retina. *The British journal of ophthalmology* 1999; **83**: 1241-1245
23. Seymenoglu G, Baser E, Ozturk B. Comparison of spectral-domain optical coherence tomography and Heidelberg retina tomograph III optic nerve head parameters in glaucoma. *Ophthalmologica* 2013; **229**: 101-105
24. Chan EW, Liao J, Wong R, Loon SC, Aung T, Wong TY, Cheng CY. Diagnostic Performance of the ISNT Rule for Glaucoma Based on the Heidelberg Retinal Tomograph. *Translational vision science & technology* 2013; **2**: 2
25. Elsner AE, Burns SA, Hughes GW, Webb RH. Reflectometry with a scanning laser ophthalmoscope. *Applied optics* 1992; **31**: 3697-3710
26. Remky A, Beausencourt E, Elsner AE. Angioscotometry with the scanning laser ophthalmoscope. Comparison of the effect of different wavelengths. *Invest Ophthalmol Vis Sci* 1996; **37**: 2350-2355
27. Remky A, Elsner AE, Morandi AJ, Beausencourt E, Trempe CL. Blue-on-yellow perimetry with a scanning laser ophthalmoscope: small alterations in the central macula with aging. *Journal of the Optical Society of America A, Optics, image science, and vision* 2001; **18**: 1425-1436
28. Hammer DX, Ferguson RD, Magill JC, White MA, Elsner AE, Webb RH. Compact scanning laser ophthalmoscope with high-speed retinal tracker. *Applied optics* 2003; **42**: 4621-4632
29. Liang J, Williams DR, Miller DT. Supernormal vision and high-resolution retinal imaging through adaptive optics. *Journal of the Optical Society of America A, Optics, image science, and vision* 1997; **14**: 2884-2892
30. Roorda A, Williams DR. The arrangement of the three cone classes in the living human eye. *Nature* 1999; **397**: 520-522
31. Roorda A, Romero-Borja F, Donnelly Iii W, Queener H, Hebert T, Campbell M. Adaptive optics scanning laser ophthalmoscopy. *Optics express* 2002; **10**: 405-412
32. Zhang Y, Roorda A. Evaluating the lateral resolution of the adaptive optics scanning laser ophthalmoscope. *Journal of biomedical optics* 2006; **11**: 014002
33. Dubra A, Sulai Y, Norris JL, Cooper RF, Dubis AM, Williams DR, Carroll J. Noninvasive imaging of the human rod photoreceptor mosaic using a confocal adaptive optics scanning ophthalmoscope. *Biomedical optics express* 2011; **2**: 1864-1876
34. Carroll J. Adaptive optics retinal imaging: applications for studying retinal degeneration. *Archives of ophthalmology (Chicago, Ill: 1960)* 2008; **126**: 857-858
35. Tam J, Tiruveedhula P, Roorda A. Characterization of single-file flow through human retinal parafoveal capillaries using an adaptive optics scanning laser ophthalmoscope. *Biomedical optics express* 2011; **2**: 781-793
36. Tam J, Martin JA, Roorda A. Noninvasive visualization and analysis of parafoveal capillaries in humans. *Invest Ophthalmol Vis Sci* 2010; **51**: 1691-1698
37. Tam J, Dhamdhare KP, Tiruveedhula P, Manzanera S, Barez S, Bearse MA Jr, Adams AJ, Roorda A. Disruption of the retinal parafoveal capillary network in type 2 diabetes before the onset of diabetic retinopathy. *Invest Ophthalmol Vis Sci* 2011; **52**: 9257-9266
38. Scoles D, Sulai YN, Dubra A. In vivo dark-field imaging of the retinal pigment epithelium cell mosaic. *Biomedical optics express* 2013; **4**: 1710-1723
39. Schutt F, Davies S, Kopitz J, Holz FG, Boulton ME. Photodamage to human RPE cells by A2-E, a retinoid component of lipofuscin. *Invest Ophthalmol Vis Sci* 2000; **41**: 2303-2308
40. Dysli C, Wolf S, Zinkernagel MS. Autofluorescence Lifetimes in Geographic Atrophy in Patients With Age-Related Macular Degeneration. *Invest Ophthalmol Vis Sci* 2016; **57**: 2479-2487
41. Parodi MB, Iacono P, Campa C, Del Turco C, Bandello F. Fundus autofluorescence patterns in Best vitelliform macular dystrophy. *Am J Ophthalmol* 2014; **158**: 1086-1092
42. Parodi MB, Iacono P, Del Turco C, Bandello F. Near-infrared fundus autofluorescence in subclinical best vitelliform macular dystrophy. *Am J Ophthalmol* 2014; **158**: 1247-1252.e1242
43. Almeida A, Kaliki S, Shields CL. Autofluorescence of intraocular tumours. *Curr Opin Ophthalmol* 2013; **24**: 222-232
44. Durrani K, Foster CS. Fundus autofluorescence imaging in posterior uveitis. *Seminars in ophthalmology* 2012; **27**: 228-235
45. Samy A, Lightman S, Ismetova F, Talat L, Tomkins-Netzer O. Role of autofluorescence in inflammatory/infective diseases of the retina and choroid. *Journal of ophthalmology* 2014; **2014**: 418193
46. Marmor MF, Kellner U, Lai TY, Melles RB, Mieler WF. Recommendations on Screening for Chloroquine and Hydroxychloroquine Retinopathy (2016 Revision). *Ophthalmology* 2016; **123**: 1386-1394
47. Schmitz-Valckenberg S, Holz FG, Bird AC, Spaide RF. Fundus autofluorescence imaging: review and perspectives. *Retina* 2008; **28**: 385-409
48. Delori FC, Dorey CK, Staurenghi G, Arend O, Goger DG, Weiter JJ. In vivo fluorescence of the ocular fundus exhibits retinal pigment epithelium lipofuscin characteristics. *Invest Ophthalmol Vis Sci* 1995; **36**: 718-729
49. Spaide RF. Fundus autofluorescence and age-related macular degeneration. *Ophthalmology* 2003; **110**: 392-399
50. Jorzik JJ, Bindewald A, Dithmar S, Holz FG. Digital simultaneous fluorescein and indocyanine green angiography, autofluorescence, and red-free imaging with a solid-state laser-based confocal scanning laser ophthalmoscope. *Retina* 2005; **25**: 405-416
51. Weinberger AW, Lappas A, Kirschkamp T, Mazinani BA, Huth JK, Mohammadi B, Walter P. Fundus near infrared fluorescence correlates with fundus near infrared reflectance. *Invest Ophthalmol Vis Sci* 2006; **47**: 3098-3108
52. Keilhauer CN, Delori FC. Near-infrared autofluorescence imaging of the fundus: visualization of ocular melanin. *Invest Ophthalmol Vis Sci* 2006; **47**: 3556-3564
53. Witmer MT, Parltitsis G, Patel S, Kiss S. Comparison of ultra-widefield fluorescein angiography with the Heidelberg Spectralis® noncontact ultra-widefield module versus the Optos® Optomap®.

- Clinical ophthalmology (Auckland, NZ)* 2013; 7: 389
54. Croft DE, van Hemert J, Wykoff CC, Clifton D, Verhoeck M, Fleming A, Brown DM. Precise montaging and metric quantification of retinal surface area from ultra-widefield fundus photography and fluorescein angiography. *Ophthalmic Surgery, Lasers and Imaging Retina* 2014; **45**: 312-317
 55. Patel M, Kiss S. Ultra-wide-field fluorescein angiography in retinal disease. *Curr Opin Ophthalmol* 2014; **25**: 213-220
 56. Reznicek L, Klein T, Wieser W, Kernt M, Wolf A, Haritoglou C, Kampik A, Huber R, Neubauer AS. Megahertz ultra-wide-field swept-source retina optical coherence tomography compared to current existing imaging devices. *Graefes archive for clinical and experimental ophthalmology = Albrecht von Graefes Archiv fur klinische und experimentelle. Ophthalmologie* 2014; **252**: 1009-1016
 57. Hashimoto H, Kishi S. Ultra-wide-field fundus autofluorescence in multiple evanescent white dot syndrome. *Am J Ophthalmol* 2015; **159**: 698-706
 58. Zapata MA, Leila M, Teixidor T, Garcia-Arumi J. Comparative study between fundus autofluorescence and red reflectance imaging of choroidal nevi using ultra-wide-field scanning laser ophthalmoscopy. *Retina* 2015; **35**: 1202-1210
 59. Tomlins PH, Wang RK. Theory, developments and applications of optical coherence tomography. *Journal of Physics D: Applied Physics* 2005; **38**: 2519
 60. Drexler W, Fujimoto JG. State-of-the-art retinal optical coherence tomography. *Prog Retin Eye Res* 2008; **27**: 45-88
 61. Sull AC, Vuong LN, Price LL, Srinivasan VJ, Gorczynska I, Fujimoto JG, Schuman JS, Duker JS. Comparison of spectral/Fourier domain optical coherence tomography instruments for assessment of normal macular thickness. *Retina* 2010; **30**: 235-245
 62. Leitgeb R, Hitzinger C, Fercher A. Performance of fourier domain vs. time domain optical coherence tomography. *Optics express* 2003; **11**: 889-894
 63. de Boer JF, Cense B, Park BH, Pierce MC, Tearney GJ, Bouma BE. Improved signal-to-noise ratio in spectral-domain compared with time-domain optical coherence tomography. *Optics letters* 2003; **28**: 2067-2069
 64. Sarunic M, Choma MA, Yang C, Izatt JA. Instantaneous complex conjugate resolved spectral domain and swept-source OCT using 3x3 fiber couplers. *Optics express* 2005; **13**: 957-967
 65. Keane PA, Sadda SR. Retinal imaging in the twenty-first century: state of the art and future directions. *Ophthalmology* 2014; **121**: 2489-2500
 66. Choma MA, Hsu K, Izatt JA. Swept source optical coherence tomography using an all-fiber 1300-nm ring laser source. *Journal of biomedical optics* 2005; **10**: 44009
 67. Keane PA, Ruiz-Garcia H, Sadda SR. Clinical applications of long-wavelength (1,000-nm) optical coherence tomography. *Ophthalmic surgery, lasers & imaging: the official journal of the International Society for Imaging in the Eye* 2011; **42 Suppl**: S67-74
 68. Steiner P, Ebner A, Berger LE, Zinkernagel M, Považay B, Meier C, Kowal JH, Framme C, Brinkmann R, Wolf S, Sznitman R. Time-Resolved Ultra-High Resolution Optical Coherence Tomography for Real-Time Monitoring of Selective Retina Therapy. *Invest Ophthalmol Vis Sci* 2015; **56**: 6654-6662
 69. Shoji T, Kuroda H, Suzuki M, Baba M, Araie M, Yoneya S. Three-dimensional optic nerve head images using optical coherence tomography with a broad bandwidth, femtosecond, and mode-locked laser. *Graefes archive for clinical and experimental ophthalmology = Albrecht von Graefes Archiv fur klinische und experimentelle. Ophthalmologie* 2015; **253**: 313-321
 70. Wang Y, Jiang H, Shen M, Lam BL, DeBuc DC, Ye Y, Li M, Tao A, Shao Y, Wang J. Quantitative analysis of the intraretinal layers and optic nerve head using ultra-high resolution optical coherence tomography. *Journal of biomedical optics* 2012; **17**: 066013
 71. Mallipatna A, Vinekar A, Jayadev C, Dabir S, Sivakumar M, Krishnan N, Mehta P, Berendschot T, Yadav NK. The use of handheld spectral domain optical coherence tomography in pediatric ophthalmology practice: Our experience of 975 infants and children. *Indian journal of ophthalmology* 2015; **63**: 586
 72. Diner O, Aksoy Y, Kaya A, Sevinç MK. Handheld spectral domain optical coherence tomography seems to be a must-have device for future treatment methods of hereditary maculopathies. *Indian journal of ophthalmology* 2016; **64**: 171
 73. Moore AT. Handheld OCT Comes of Age. *Investigative ophthalmology & visual science* 2015; **56**: 4546-4546
 74. Nankivil D, Waterman G, LaRocca F, Keller B, Kuo AN, Izatt JA. Handheld, rapidly switchable, anterior/posterior segment swept source optical coherence tomography probe. *Biomedical optics express* 2015; **6**: 4516-4528
 75. Goldberg RA, Waheed NK, Duker JS. Optical coherence tomography in the preoperative and postoperative management of macular hole and epiretinal membrane. *British Journal of Ophthalmology, bjophthalmol* 2013 (2014).
 76. Riazi-Esfahani M, Khademi MR, Mazloumi M, Khodabandeh A, Riazi-Esfahani H. Macular surgery using intraoperative spectral domain optical coherence tomography. *Journal of ophthalmic & vision research* 2014; **10**: 309
 77. Ehlers JP, Han J, Petkovsek D, Kaiser PK, Singh RP, Srivastava SK. Membrane Peeling-Induced Retinal Alterations on Intraoperative OCT in Vitreomacular Interface Disorders From the PIONEER Study Membrane Peeling-Induced Retinal Alterations. *Investigative ophthalmology & visual science* 2015; **56**: 7324-7330
 78. Mura M, Iannetta D, Nasini F, Barca F, Peiretti E, Engelbrecht L, de Smet MD, Verbraak F. Use of a new intra-ocular spectral domain optical coherence tomography in vitreoretinal surgery. *Acta ophthalmologica*, (2016).
 79. Leitgeb RA, Schmetterer L, Drexler W, Fercher A, Zawadzki R, Bajraszewski T. Real-time assessment of retinal blood flow with ultrafast acquisition by color Doppler Fourier domain optical coherence tomography. *Optics Express* 2003; **11(23)**: 3116-3121
 80. Werkmeister RM, Dragostinoff N, Pircher M, Götzinger E, Hitzinger CK, Leitgeb RA, Schmetterer L. Bidirectional Doppler Fourier-domain optical coherence tomography for measurement of absolute flow velocities in human retinal vessels. *Optics letters* 2008; **33**: 2967-2969
 81. Blatter C, Grajciar B, Schmetterer L, Leitgeb RA. Angle independent flow assessment with bidirectional Doppler optical coherence tomography. *Optics letters* 2013; **38**: 4433-4436
 82. Lee B, Choi W, Liu JJ, Lu CD, Schuman JS, Wollstein G, Duker JS, Waheed NK, Fujimoto JG. Cardiac-Gated En Face Doppler Measurement of Retinal Blood Flow Using Swept-Source Optical Coherence Tomography at 100,000 Axial Scans per Second. *Invest Ophthalmol Vis Sci* 2015; **56**: 2522-2530
 83. Jia Y, Tan O, Tokayer J, Potsaid B, Wang Y, Liu JJ, Kraus MF, Subhash H, Fujimoto JG, Hornegger J, Huang D. Split-spectrum amplitude-decorrelation angiography with optical coherence tomography. *Optics express* 2012; **20**: 4710-4725
 84. Coscas G, Lupidi M, Coscas F. Image Analysis of Optical Coherence Tomography Angiography. In: *OCT Angiography in Retinal and Macular Diseases*. Karger Publishers (2016).
 85. Blatter C, Klein T, Grajciar B, Schmoll T, Wieser W, Andre R, Huber R, Leitgeb RA. Ultrahigh-speed non-invasive widefield angiography. *Journal of biomedical optics* 2012; **17**: 0705051-0705053
 86. de Carlo TE, Romano A, Waheed NK, Duker JS. A review of optical coherence tomography angiography (OCTA). *International Journal of Retina and Vitreous* 2015; **1**: 1
 87. Huang D, Jia Y, Gao SS, Lumbroso B, Rispoli M. Optical Coherence Tomography Angiography Using the Optovue Device. In: *OCT Angiography in Retinal and Macular Diseases*. Karger Pub-

- lishers (2016).
88. Hwang TS, Jia Y, Gao SS, Bailey ST, Lauer AK, Flaxel CJ, Wilson DJ, Huang D. Optical coherence tomography angiography features of diabetic retinopathy. *Retina (Philadelphia, PA)* 2015; **35**: 2371
 89. Ishibazawa A, Nagaoka T, Takahashi A, Omae T, Tani T, Sogawa K, Yokota H, Yoshida A. Optical coherence tomography angiography in diabetic retinopathy: a prospective pilot study. *American journal of ophthalmology* 2015; **160**: 35-44
 90. Talisa E, Chin AT, Bonini Filho MA, Adhi M, Branchini L, Salz DA, Bauman CR, Crawford C, Reichel E, Witkin AJ, Duker JS, Waheed NK. Detection of microvascular changes in eyes of patients with diabetes but not clinical diabetic retinopathy using optical coherence tomography angiography. *Retina* 2015; **35**: 2364-2370
 91. Agemy SA, Scripsema NK, Shah CM, Chui T, Garcia PM, Lee JG, Gentile RC, Hsiao YS, Zhou Q, Ko T, Rosen RB. Retinal vascular perfusion density mapping using optical coherence tomography angiography in normals and diabetic retinopathy patients. *Retina* 2015; **35**: 2353-2363
 92. Palejwala NV, Witkin AJ, Ko TH, Fujimoto JG, Chan A, Schuman JS, Ishikawa H, Reichel E, Duker JS. Detection of non-exudative choroidal neovascularization in age-related macular degeneration with optical coherence tomography angiography. *Retina (Philadelphia, PA)* 2015; **35**: 2204
 93. El Ameen A, Cohen SY, Semoun O, Miere A, Srour M, Quarantel El Maftouhi M, Oubrahim H, Blanco-Garavito R, Querques G, Souied EH. Type 2 neovascularization secondary to age-related macular degeneration imaged by optical coherence tomography angiography. *Retina* 2015; **35**: 2212-2218
 94. Kuehlewein L, Dansingani KK, de Carlo TE, Bonini Filho MA, Iafe NA, Lenis TL, Freund KB, Waheed NK, Duker JS, Sadda SR, Sarraf D. Optical coherence tomography angiography of type 3 neovascularization secondary to age-related macular degeneration. *Retina* 2015; **35**: 2229-2235
 95. Toto L, Borrelli E, Di Antonio L, Carpineto P, Mastropasqua R. Retinal vascular plexuses' changes in dry age-related macular degeneration, evaluated by means of optical coherence tomography angiography. *Retina (Philadelphia, PA)*, (2016).
 96. Waheed NK, Moulton EM, Fujimoto JG, Rosenfeld PJ. Optical Coherence Tomography Angiography of Dry Age-Related Macular Degeneration. In: *OCT Angiography in Retinal and Macular Diseases*. Karger Publishers (2016).
 97. Kashani AH, Lee SY, Moshfeghi A, Durbin MK, Puliafito CA. Optical coherence tomography angiography of retinal venous occlusion. *Retina* 2015; **35**: 2323-2331
 98. Spaide RF. Optical coherence tomography angiography signs of vascular abnormalization with antiangiogenic therapy for choroidal neovascularization. *American journal of ophthalmology* 2015; **160**: 6-16
 99. Muakkassa NW, Chin AT, de Carlo T, Klein KA, Bauman CR, Witkin AJ, Duker JS, Waheed NK. Characterizing the effect of anti-vascular endothelial growth factor therapy on treatment-naive choroidal neovascularization using optical coherence tomography angiography. *Retina* 2015; **35**: 2252-2259
 100. Zeimer M, Gutfleisch M, Heimes B, Spital G, Lommatzsch A, Pauleikhoff D. Association between changes in macular vasculature in optical coherence tomography- and fluorescein-angiography and distribution of macular pigment in type 2 idiopathic macular telangiectasia. *Retina* 2015; **35**: 2307-2316
 101. Han IC, Tadarati M, Scott AW. Macular vascular abnormalities identified by optical coherence tomographic angiography in patients with sickle cell disease. *JAMA ophthalmology* 2015; **133**: 1337-1340
 102. Bonini Filho MA, de Carlo TE, Ferrara D, Adhi M, Bauman CR, Witkin AJ, Reichel E, Duker JS, Waheed NK. Association of choroidal neovascularization and central serous chorioretinopathy with optical coherence tomography angiography. *JAMA ophthalmology* 2015; **133**: 899-906
 103. Liu L, Jia Y, Takusagawa HL, Pechauer AD, Edmunds B, Lombardi L, Davis E, Morrison JC, Huang D. Optical coherence tomography angiography of the peripapillary retina in glaucoma. *JAMA ophthalmology*, (2015).
 104. Wang LV, Hu S. Photoacoustic tomography: in vivo imaging from organelles to organs. *Science (New York, NY)* 2012; **335**: 1458-1462
 105. Hu Z, Wang X, Liu Q, Paulus YM. Photoacoustic Imaging in Ophthalmology. *Int J Ophthalmol Eye Res* 2015; **3**: 126-132
 106. Silverman RH, Kong F, Chen YC, Lloyd HO, Kim HH, Cannata JM, Shung KK, Coleman DJ. High-resolution photoacoustic imaging of ocular tissues. *Ultrasound in medicine & biology* 2010; **36**: 733-742
 107. de la Zerma A, Paulus YM, Teed R, Bodapati S, Dollberg Y, Khuri-Yakub BT, Blumenkranz MS, Moshfeghi DM, Gambhir SS. Photoacoustic ocular imaging. *Optics letters* 2010; **35**: 270-272
 108. Liu X, Liu T, Wen R, Li Y, Puliafito CA, Zhang HF, Jiao S. Optical coherence photoacoustic microscopy for in vivo multimodal retinal imaging. *Optics letters* 2015; **40**: 1370-1373
 109. Jiao S, Jiang M, Hu J, Fawzi A, Zhou Q, Shung KK, Puliafito CA, Zhang HF. Photoacoustic ophthalmoscopy for in vivo retinal imaging. *Optics express* 2010; **18**: 3967-3972
 110. Song W, Wei Q, Jiao S, Zhang HF. Integrated photoacoustic ophthalmoscopy and spectral-domain optical coherence tomography. *JoVE (Journal of Visualized Experiments)*, 2013; e4390-e4390
 111. Liu T, Li H, Song W, Jiao S, Zhang HF. Fundus camera guided photoacoustic ophthalmoscopy. *Current eye research* 2013; **38**: 1229-1234
 112. Zhang X, Zhang HF, Puliafito CA, Jiao S. Simultaneous in vivo imaging of melanin and lipofuscin in the retina with photoacoustic ophthalmoscopy and autofluorescence imaging. *Journal of biomedical optics* 2011; **16**: 080504-080504
 113. Zhang X, Jiang M, Fawzi AA, Li X, Shung KK, Puliafito CA, Zhang HF, Jiao S. Simultaneous dual molecular contrasts provided by the absorbed photons in photoacoustic microscopy. *Optics letters* 2010; **35**: 4018-4020
 114. Song W, Wei Q, Liu W, Liu T, Yi J, Sheibani N, Fawzi AA, Linsenmeier RA, Jiao S, Zhang HF. A combined method to quantify the retinal metabolic rate of oxygen using photoacoustic ophthalmoscopy and optical coherence tomography. *Scientific reports* 2014; **4**: 6525
 115. Cordeiro MF, Guo L, Luong V, Harding G, Wang W, Jones HE, Moss SE, Sillito AM, Fitzke FW. Real-time imaging of single nerve cell apoptosis in retinal neurodegeneration. *Proceedings of the National Academy of Sciences of the United States of America* 2004; **101**: 13352-13356
 116. Coxon KM, Duggan J, Cordeiro MF, Moss SE. Purification of annexin V and its use in the detection of apoptotic cells. *Methods in molecular biology (Clifton, NJ)* 2011; **731**: 293-308
 117. Barnett EM, Zhang X, Maxwell D, Chang Q, Piwnica-Worms D. Single-cell imaging of retinal ganglion cell apoptosis with a cell-penetrating, activatable peptide probe in an in vivo glaucoma model. *Proceedings of the National Academy of Sciences of the United States of America* 2009; **106**: 9391-9396
 118. Dickinson BC, Tang Y, Chang Z, Chang CJ. A nuclear-localized fluorescent hydrogen peroxide probe for monitoring sirtuin-mediated oxidative stress responses in vivo. *Chemistry & biology* 2011; **18**: 943-948
 119. Vrabcic JP, Lieven CJ, Levin LA. Cell-type-specific opening of the retinal ganglion cell mitochondrial permeability transition pore. *Invest Ophthalmol Vis Sci* 2003; **44**: 2774-2782
 120. Okubo Y, Sekiya H, Namiki S, Sakamoto H, Iinuma S, Yamasaki M, Watanabe M, Hirose K, Iino M. Imaging extrasynaptic glutamate dynamics in the brain. *Proceedings of the National Academy of Sciences of the United States of America* 2010; **107**: 6526-6531
 121. King A, Gottlieb E, Brooks DG, Murphy MP, Dunaief JL. Mi-

- tochondria-derived reactive oxygen species mediate blue light-induced death of retinal pigment epithelial cells. *Photochemistry and photobiology* 2004; **79**: 470-475
122. Hageman GS, Luthert PJ, Victor Chong NH, Johnson LV, Anderson DH, Mullins RF. An integrated hypothesis that considers drusen as biomarkers of immune-mediated processes at the RPE-Bruch's membrane interface in aging and age-related macular degeneration. *Prog Retin Eye Res* 2001; **20**: 705-732
123. Takeda A, Baffi JZ, Kleinman ME, Cho WG, Nozaki M, Yamada K, Kaneko H, Albuquerque RJ, Dridi S, Saito K, Raisler BJ, Budd SJ, Geisen P, Munitz A, Ambati BK, Green MG, Ishibashi T, Wright JD, Humbles AA, Gerard CJ, Ogura Y, Pan Y, Smith JR, Grisanti S, Hartnett ME, Rothenberg ME, Ambati J. CCR3 is a target for age-related macular degeneration diagnosis and therapy. *Nature* 2009; **460**: 225-230
124. Grisanti S, Canbek S, Kaiserling E, Adam A, Lafaut B, Gelisken F, Szurman P, Henke-Fahle S, Oficjalska-Mlynczak J, Bartz-Schmidt KU. Expression of endoglin in choroidal neovascularization. *Exp Eye Res* 2004; **78**: 207-213
125. Peiris PM, Toy R, Doolittle E, Pansky J, Abramowski A, Tam M, Vicente P, Tran E, Hayden E, Camann A, Mayer A, Erokwu BO, Berman Z, Wilson D, Baskaran H, Flask CA, Keri RA, Karathanasis E. Imaging metastasis using an integrin-targeting chain-shaped nanoparticle. *ACS nano* 2012; **6**: 8783-8795
126. Li F, Liu J, Jas GS, Zhang J, Qin G, Xing J, Cotes C, Zhao H, Wang X, Diaz LA, Shi ZZ, Lee DY, Li KC, Li Z. Synthesis and evaluation of a near-infrared fluorescent non-peptidic bivalent integrin $\alpha(v)\beta(3)$ antagonist for cancer imaging. *Bioconjugate chemistry* 2010; **21**: 270-278

Peer reviewer: Ali Osman Saatci Professor, MD, Mustafa Kemal Sahil Bulvari No.73, A Blok,Daire 9, Narlidere,İzmir,Turkey.